2026 IEEE/SICE International Symposium on System Integration (SII)
January 11-14, 2026. Cancún, México

Real-Time Fingertip Force Estimation from Lateral Deformation for Precision Manipulation Task

Jiang Shixuan, and Atsutoshi Ikeda, *Member, IEEE*

Abstract— **This study proposes a wearable fingertip force estimation approach that employs a single three-axis force sensor mounted on the side of the fingernail, enabling measurements under natural contact conditions without obscuring the fingerpad. Fingertip deformation during contact is captured by the sensor, and calibration experiments are performed using a table-mounted force sensor to relate the measured lateral deformation to actual normal and tangential forces. Two modeling approaches—a 6th-order multi-input multi-output transfer function model and an 8th-order state-space model—are identified from the calibration data. The transfer function model achieves high offline accuracy ($R^2 \approx 0.9$, RMSE ≤ 7%FS), while the state-space model offers smoother, low-latency output suitable for real-time feedback. These results clarify the relationship between fingertip deformation and applied forces, providing a scientific basis for improving skill transfer, training protocols, and haptic simulation in precision manual tasks.**

I. Introduction

The human fingertip is densely populated with tactile receptors, and the mechanical information captured by mechanoreceptors plays a crucial role in gripping and manipulating objects. In precision assembly and machining, highly skilled workers rely on fingertip sensations to adjust applied forces and to judge work quality. However, such tactile skills depend heavily on personal experience and subjective judgment, posing challenges for skill transfer and instruction. Advances in tactile sensing and measurement technologies offer new ways to address this issue.

Finger-pad deformation during contact events is typically analyzed with 2-D or 3-D computational models [1]. For example, multilayer 3-D finite-element models have been used to examine stress and strain at receptor locations [2]; simplified fingernail-shell models can efficiently simulate surface deformation of the finger pad [3]; and 3-D beam-bundle models have been applied to simulate fingertip interactions during pressing and sliding on a plane [4]. These studies explore, at a theoretical level, the relationship between tissue deformation of the finger pad and the forces exerted.

In this work, a single three-axis tactile force sensor is used to investigate fingertip force regulation and deformation perception under natural contact conditions (Fig.1). Calibration experiments in conjunction with a table-mounted tri-axial force sensor to simulate finger-pad pressing under various conditions [5], establish a direct link between lateral forces and actual finger-pad deformation, and employ transfer-function and state-space models to predict both deformation and force [6].

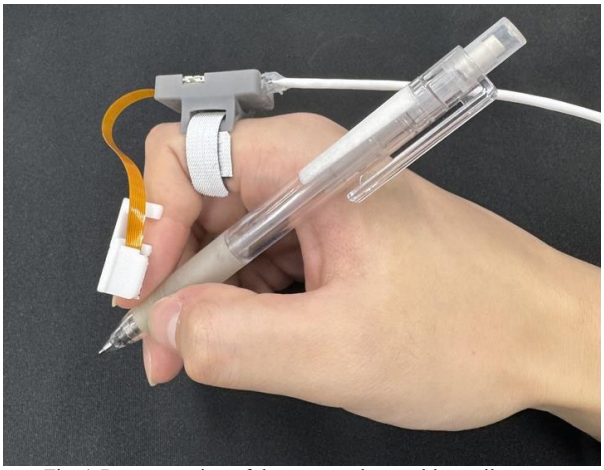

Fig. 1 Demonstration of the proposed wearable tactile sensor in a writing task

The objective, compared with earlier studies, is to develop a system that relies on just one lateral tactile sensor, accurately measures finger-pad deformation without disturbing natural manipulation, and maintains a high degree of mounting freedom while minimizing interference with the contact surface. The prediction framework captures dynamic characteristics more effectively by adopting both transfer-function and state-space system-identification approaches, enabling model accuracy to be optimized across different contact scenarios. This capability is critical for enhancing the reliability and accuracy of tactile feedback in high-precision manual tasks such as micro-assembly, conservation of cultural artifacts, and surgical procedures. The anticipated applications of this technology will deepen understanding of human tactile mechanisms, provide practical tools for skill assessment and education, and facilitate effective skill.

The following sections will describe the hardware of the FLD sensor and the principles behind measuring lateral fingertip deformation and forces. The method for estimating

This Research is supported by the New Energy and Industrial Technology Development Organization (NEDO).
Jiang Shixuan is with the Graduate School of Science and Engineering, Kindai University, Osaka, Japan 2433330361h@kindai.ac.jp

Atsutoshi Ikeda is with the Graduate School of Science and Engineering, Kindai University, Osaka, Japan, ikeda@emat.kindai.ac.jp
https://orcid.org/0000-0002-7380-4048

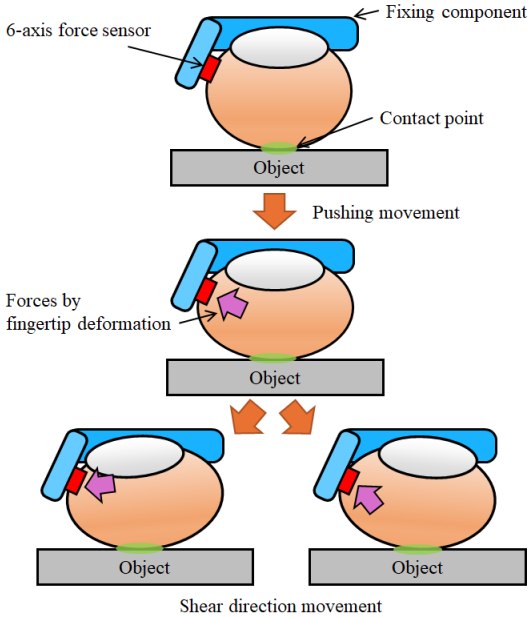

Fig. 2 Estimation results of lateral shear stress

fingertip deformation and forces will be detailed in Section III, while the experimental setup and results for validating the proposed method will be presented in Section IV.

II. FINGERTIP LATERAL DEFORMATION SENSOR

Fig. 2 shows a conceptual image of the proposed fingertip deformation measurement using a single sensor. Upon contact with an object, the fingertip undergoes lateral expansion due to the application of a normal force. As the normal force increases, the fingertip deforms further, generating reaction forces at the contact interface. When a tangential force is introduced, the deformation becomes asymmetric, with the lateral displacement on the side in the direction of the tangential force being smaller than that on the opposite side. This asymmetric deformation persists until the fingertip reaches the point of slipping. The extent of lateral deformation is influenced by multiple factors, including the mechanical properties of the fingertip (e.g., shape, size, and stiffness), the magnitude of the normal and tangential forces, and the frictional characteristics of the contact surface. These findings suggest that by developing a model of fingertip mechanical deformation, it is possible to infer the normal force, tangential force, and friction based on observed lateral deformation patterns.

The fixing component is designed so that the 3-axis force sensor would be the side of the fingernail. This is to avoid interference with the object and other fingers, which is an advantage of the proposed device. According to our preliminary experiments, the side of the fingernail is the second most deformed area due to fingertip contact after the lateral side of the finger pad. Thus, this location is considered to be suitable for the sensor layout.

The fixing component for attaching the sensor on the finger is the most important part. If the relative position of the sensor and the finger changes during the measurement, the fingertip force estimation will be greatly affected. In addition, it must be rigid enough not to deform even when subjected to forces

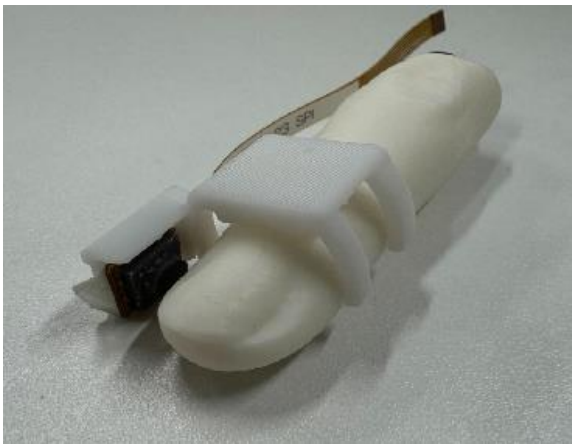

Fig. 3 Tactile sensor and fixture designed for measurements.

caused by deformation of the fingertip. On the other hand, the shape must be such that it does not interfere with the work. In this paper, the size and shape of the fixing component were determined based on the subject's finger shape, which was measured in detail. The fixing component has the shape of a C-shaped ring and is mounted to the beginning of the distal phalanx and the end of the middle phalanx of the index finger (across the distal inter phalangeal joint).

The sensor attachment is integrated with the fixing component and can be designed to fit either side of the finger. By fixing the distal phalanx side more tightly than the middle phalanx side, the measurement device follows the movement of the distal phalanx; this is not suitable for tasks in which the DIP joint bends significantly and is an issue for future work. The fixing component was 3D printed.

To measure the deformation and force of the fingertip when contacting objects, the Shokac chip T08 (T08R1-WM155-K1-C1X) from Touchence has been adopted. This triaxial force tactile sensor can record real-time pressure on the Z-axis and shear stress changes on the X and Y axes at the sensor contact points, thus capturing the lateral deformation and force changes of the fingertip during contact events.

Overall, this sensing device provides a powerful tool for understanding and quantifying human tactile responses during precision operations. This is crucial for improving product design, enhancing user experience, and developing new tactile feedback systems.

III. MODEL FOR FINGERTIP FORCE ESTIMATION

A. *Transfer Function Model*

In this work, a transfer-function (TF) model is used to convert strain-gauge signals into fingertip force estimates. Treating the human fingertip and the FLD sensor as a single haptic-sensing system, the TF approach links measured lateral deformation directly to normal and tangential forces at the fingerpad.

The system has three inputs—the tri-axial forces recorded by the side sensor (*Fx, Fy, Fz (N)*), and produces three outputs, the predicted fingertip forces(*Yx, Yy, Yz(N)*) In the Laplace domain the relationship is:

$$Y(s) = G(s)U(s) \quad (1)$$

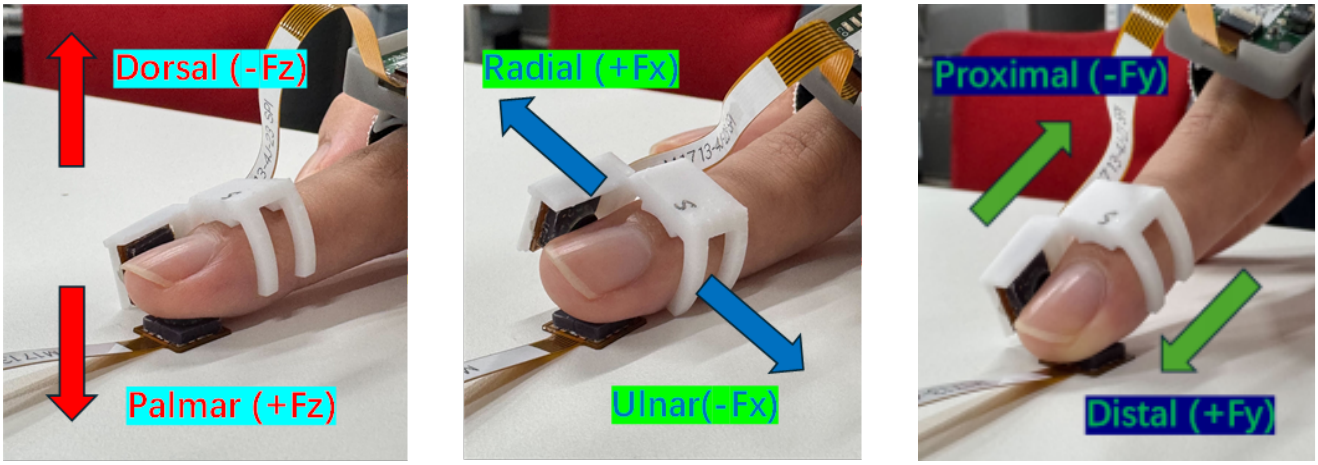

Fig. 4 Calibration experimental setup

where U(s) is the input vector, Y(s) the output vector, and G(s) a 3×3 transfer matrix:

$$U(s) = \begin{pmatrix} F_x(s) \\ F_y(s) \\ F_z(s) \end{pmatrix} \tag{2}$$

$$G(s) = \begin{pmatrix} G_{xx}(s) & G_{yx}(s) & G_{zx}(s) \\ G_{xy}(s) & G_{yy}(s) & G_{zy}(s) \\ G_{xz}(s) & G_{yz}(s) & G_{zz}(s) \end{pmatrix} \tag{3}$$

$$Y(s) = \begin{pmatrix} Y_x(s) \\ Y_y(s) \\ Y_z(s) \end{pmatrix} \tag{4}$$

Here G(s) contains nine scalar transfer functions that capture the coupling between each input and output.

Model parameters and the pole–zero distribution are identified with MATLAB's System Identification Toolbox (MathWorks, Inc.). Using a multi-input multi-output (MIMO) framework and the recorded data set, the TF order is restricted to 4th–6th order to obtain a numerically stable yet accurate representation of fingertip dynamics.

B. State-Space model

To further capture the dynamic behavior of the fingertip force–deformation process, a state-space model is identified in addition to the transfer-function approach. Whereas a transfer function emphasizes the direct input–output mapping, the state-space model represents the system's instantaneous energy storage and release through an explicit internal state vector. This formulation remains numerically stable at 7-10th orders in this study and is well suited to real-time implementation. The space model is represented as:

$$\begin{aligned} \dot{x}(t) &= Ax(t) + Bu(t) \\ y(t) &= Cx(t) + Du(t) \end{aligned} \tag{5}$$

Where x(t) is the state vector representing the internal fingertip–sensor dynamics; u(t) is the input vector containing the tri-axial forces (*Fx,Fy,Fz*) measured by the side sensor.

y(t) is the output vector of the estimated fingertip forces (normal and tangential).

A (state), B (input), C (output), and D (feed-through) are constant matrices that characterize the system's dynamics and direct coupling.

Matrices A, B, C, D are identified from experimental data using the System Identification Toolbox in MATLAB (MathWorks, Inc.). A multi-input multi-output (MIMO) framework is adopted, and the model order is restricted to 7–10 states to balance numerical stability with fidelity. For real-time implementation, the continuous model is discretized with the sampling period Ts=0.1 s (10 Hz) before being deployed to predict fingertip forces frame by frame.

IV. Experimental Setup and Estimation Result

A. Experimental Setup

To accurately relate lateral input forces to fingertip output forces, a calibration experiment was conducted. Three participants each completed three runs, yielding nine data sets. Two tactile sensors were employed: one mounted on the lateral side of the fingertip and the other fixed to a horizontal tabletop. While pressing the tabletop sensor, forces from both sensors were synchronously recorded (Fig. 4).

To mimic realistic manipulation and increase data diversity, the calibration covered the six principal motion axes illustrated in (Fig. 4):

Palmar (+*Fz*) and Dorsal (–*Fz*) vertical presses.

Radial (+*Fx*) and Ulnar (–*Fx*) lateral tilts and movemnt.

Distal (+*Fy*) and Proximal (–*Fy*) longitudinal tilts and movement.

Each single-axis [7] press lasted about 15 s. After these six trials, an additional 15 s "combined" trial blended vertical and lateral components to emulate multi-directional contact. To

curb over-fitting and provide an unbiased performance check, 80 % of the samples were randomly assigned to the training set and the remaining 20 % to the validation set. All signals were captured at 10 Hz without filtering to preserve their native characteristics. After temporal alignment, the data were used to derive an initial transfer-function model that underpins subsequent force-prediction experiments.

According to previous studies [8][9], the performance of a prediction model can be assessed with two categories of metrics: performance of fit and error. This work uses the coefficient of determination (R^2) and Pearson's correlation coefficient (Corr/r) to quantify how well the model explains variance and linear trends, while the root-mean-square error (RMSE) and mean absolute error (MAE) are adopted to measure absolute deviations. The formulas are presented as:

$$R^2 = 1 - \frac{\sum_{i=1}^{N}(y_i - \hat{y}_i)^2}{\sum_{i=1}^{N}(y_i - \bar{y})^2} \tag{6}$$

$$r(Corr) = \frac{\sum_{i=1}^{N}(y_i - \bar{y})(\hat{y}_i - \bar{\hat{y}})}{\sqrt{\sum_{i=1}^{N}(y_i - \bar{y})^2}\sqrt{\sum_{i=1}^{N}(\hat{y}_i - \bar{\hat{y}})^2}} \tag{7}$$

Here, y_i denotes the measured value, $\hat{y}_i$ the model prediction, $\bar{y}$and $\bar{\hat{y}}$ the corresponding means, and N the sample size. In general, smaller RMSE/MAE and R^2,|r|(Corr) values closer to 1 indicate higher accuracy and a better fit. All

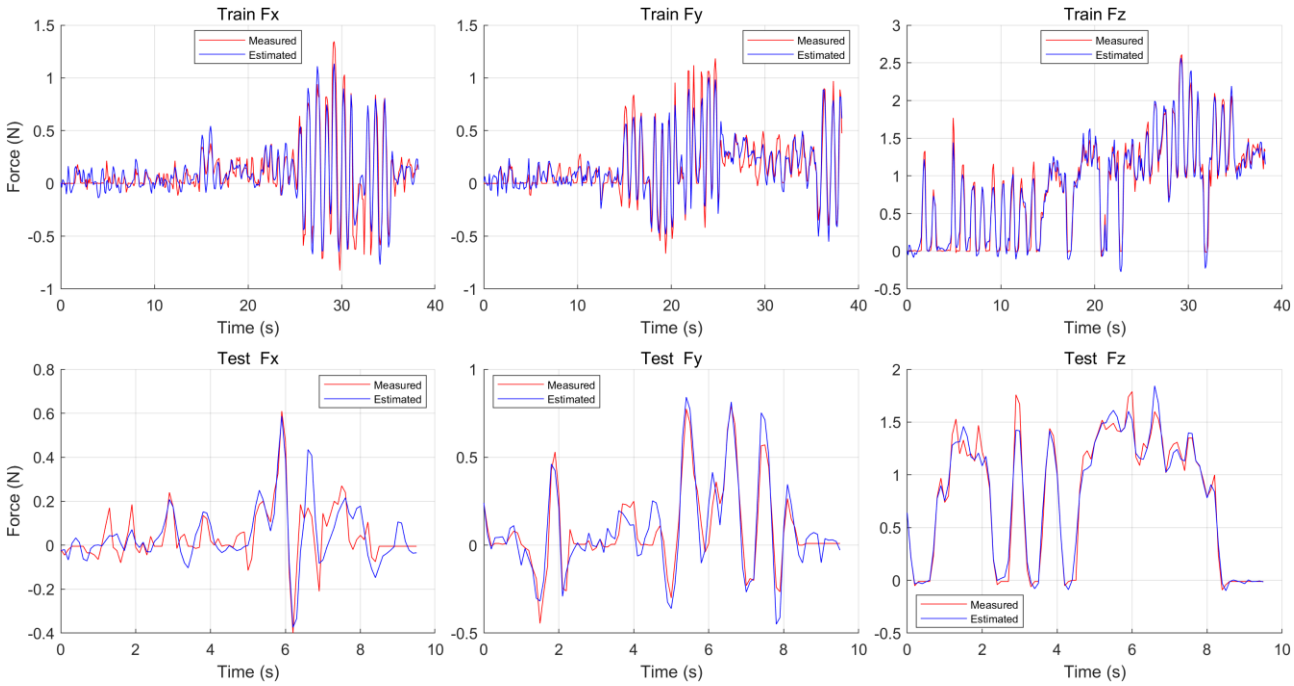

Fig. 5 Transfer function estimation results in 6th order（P1）

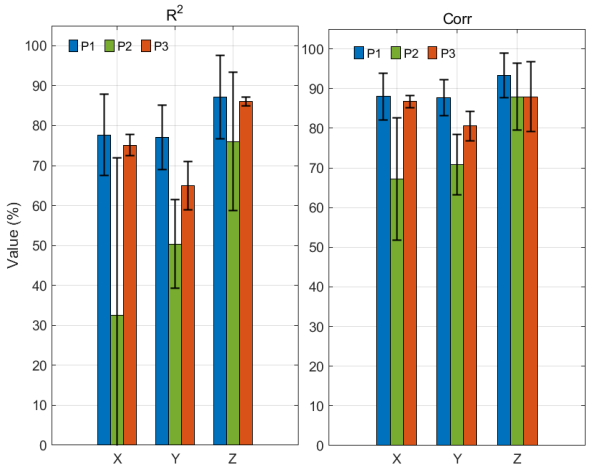

Fig. 6 coefficient of determination& Pearson correlation coefficient results of 3 participants

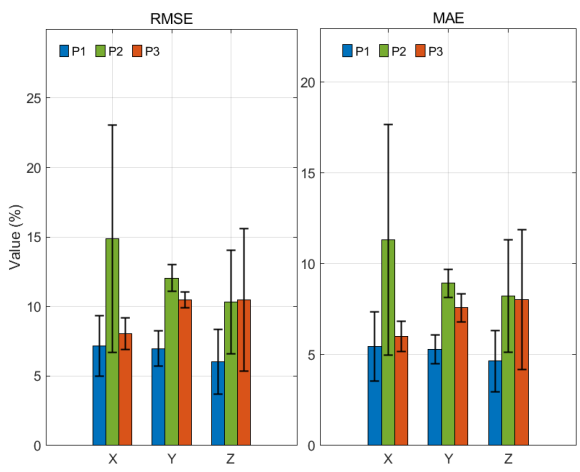

Fig. 7 Root Mean Square Error& Mean Absolute Error of 3 participants

subsequent results and discussion in this paper are based on these four metrics.

The purpose of this experimental design was to provide experimental data for the initial construction of a force prediction model and to establish a basis for further research. The repetition of experiments and the control of trial duration were designed to enhance the stability of the model and prevent prediction errors due to data bias or overfitting.

B. Transfer Function Estimation Result

In the training phase with the 6th-order transfer-function model (Fig.5), the estimated curves almost overlap the measured traces; peaks, troughs, and phase align closely, indicating that six poles and zeros are sufficient to capture the dominant dynamics of the fingertip–side-sensor system. In the 10s independent test segment (Fig.5), trends and amplitudes for the Fx and Fz components remain in good agreement, with only minor phase lag at a few sharp peaks. By contrast, the Fy component shows slight underestimation of peaks and some low-frequency drift, suggesting lower sensitivity in the shear channel and the need for further refinement.

The numerical metrics quantify these observations. Across the three participants, the coefficient of determination R^2 ranges from 0.80 to 0.92, and the absolute Pearson correlation Corr stays near 0.90, confirming that the model captures the linear relationships of all three force axes well. The Z axis (normal force) performs best, followed by X; the Y axis is slightly weaker but still explains more than 60 % of the variance (Fig. 6).

Error indices(RMSE and MAE)are normalized to the full-scale (FS) range: RMSE for the X, Y, and Z axes is generally held within 10 %FS, with the Z axis lowest and X and Y somewhat higher; MAE is below 10 % FS for all axes, with

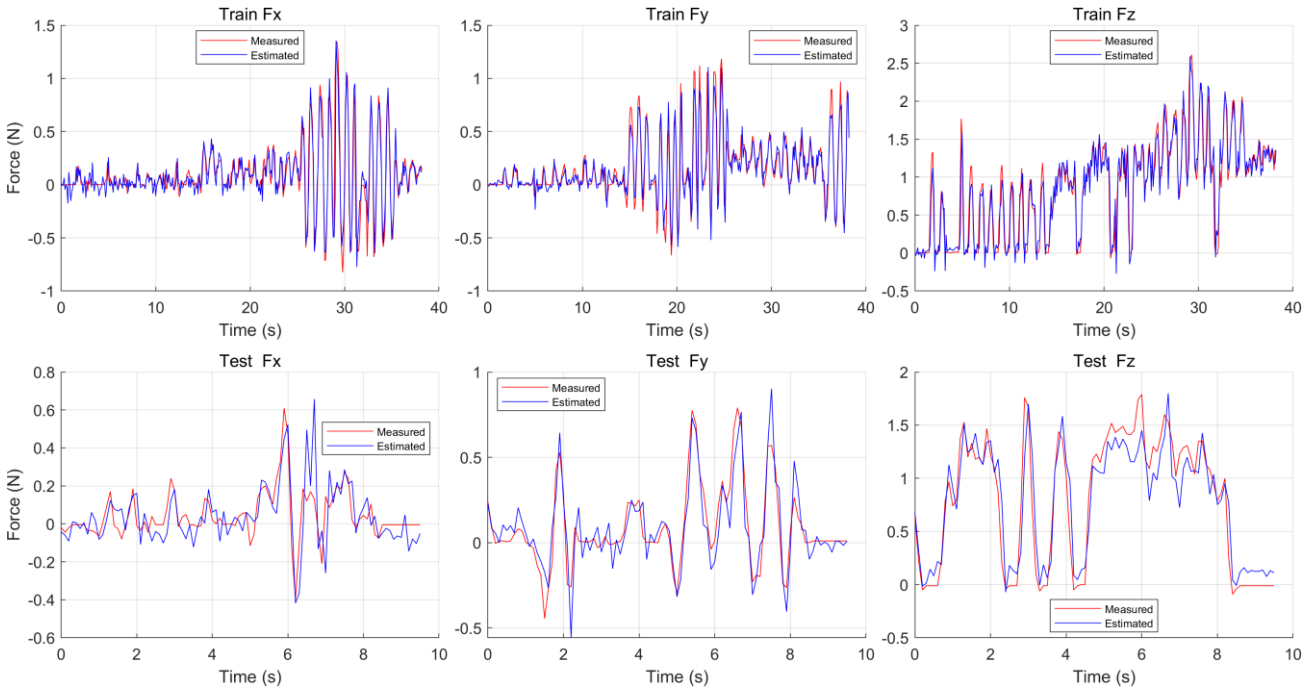

Fig. 8 space model estimation results in 8th order（P1）

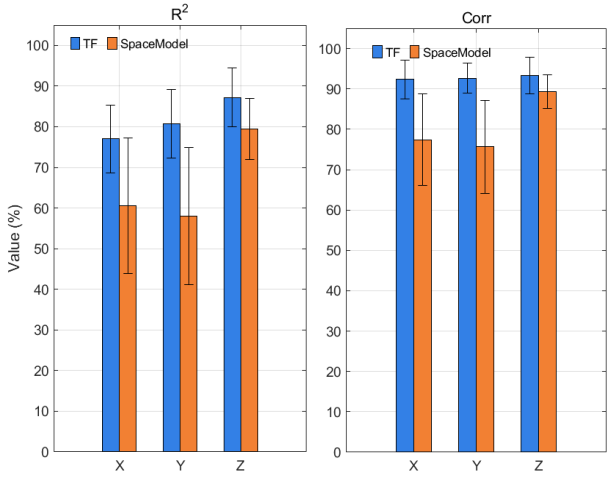

Fig. 9 Comparison of TF and SS models: R² and Pearson *r* (P1)

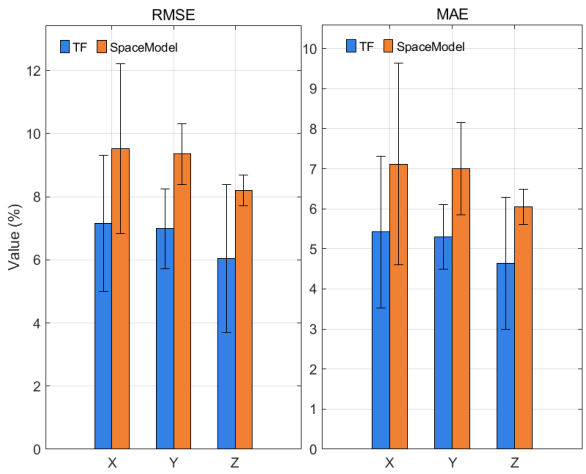

Fig. 10 Comparison of TF and SS models: RMSE and MAE (P1)

the Z-axis error for participant P1 dropping to about 5 %FS, indicating that most residuals can be regarded as acceptable random noise. Participant (P2) shows slightly poorer and error values overall, likely due to fixture fit differences and small calibration offsets (Fig.7).

Overall, the 6th-order transfer-function model can predict the tri-axial fingertip forces with errors no greater than 10 % FS and correlations above 0.80, meeting the accuracy requirements for practical fingertip force estimation. ability and complexity, avoiding both overfitting and underfitting.

C. State-Space Model Estimation Results

For the same participant (P1) used in the TF analysis, an 8-th-order state-space (SS) model was trained and evaluated. During the 40 s training segment (Fig. 8) the predicted curves closely track the measured forces, with peak amplitudes being slightly damped by the model's internal state filtering. In the 10 s independent test segment, Fx and Fz exhibit almost no phase lag or ringing, whereas Fy shows mild peak underestimation and low-frequency drift, indicating lower shear-channel sensitivity.

Numeric metrics on P1's data support these observations. The coefficient of determination R^2, lies between 0.58 and 0.79, and the absolute Pearson correlation |r|(Corr) between 0.77 and 0.89 (Fig. 9). The Z-axis (normal force) fits best, X is moderate, and Y is weakest yet still explains over 58 % of the variance. Relative to the 6-th-order transfer-function (TF) model for the same participant, SS shows a 10–20 percentage-point reduction in both R^2, |r|(Corr), reflecting lower static accuracy.

Error metrics (Fig. 10) are normalized to full scale: RMSE: 8–10 % FS and MAE: 6–7 % FS, higher than TF's 5–7 % FS yet still below the common 10 % FS engineering limit. Longer error bars indicate greater variability and more extreme outliers. Thus, for participant P1, the SS model sacrifices some static precision but delivers smoother, low-noise, low-latency output, which can be advantageous in real-time closed-loop haptic applications.

D. Discussion

The TF model provides the highest accuracy but is computationally heavy, making it suitable for offline use. The SS model is lightweight and stable, enabling smooth real-time force estimation.

A remaining limitation is that the current calibration is performed only on flat surfaces. Fingertip deformation can change significantly with object geometry (e.g., curved, edge, or point contacts), which may affect prediction accuracy. Future tests with varied contact shapes are needed to quantify this dependence.

In addition, the present framework estimates only the net force vector. Since deformation patterns also encode where the load is applied, extending the model to estimate and reveal the center of force is a promising direction for improving manipulation analysis and haptic applications.

V. CONCLUSION

This work introduced a unilateral, wearable tactile-sensing scheme that converts lateral fingertip forces into estimates of pad deformation and shear stress. Calibration tests showed that a 6th-order MIMO transfer-function model yields high offline accuracy ($R^2 \approx 0.9$; RMSE $\leq$ 7% FS), while an 8th-order state-space model, though less precise, delivers smooth, low-latency output suitable for real-time force feedback. In addition to improving model parameters, particularly for the shear axis—and redesigning the sensor attachment to reduce inter-subject variability, future efforts will also evaluate the method under non-flat contact geometries, where deformation patterns differ from planar conditions, and explore extending the framework to estimate and reveal the center of force, enabling richer interpretation of fingertip interactions during precision manipulation.

ACKNOWLEDGMENT

This work was supported by Council for Science, Technology and Innovation, "Cross-ministerial Strategic Innovation Promotion Program (SIP), Development of foundational technologies and rules for expansion of the virtual economy" (JPJ012495). (funding agency: NEDO).

REFERENCES

[1] M. Nakatani, T. Kawasoe, K. Shiojima, K. Koketsu, S. Kinoshita and J. Wada, "Wearable contact force sensor system based on fingerpad deformation," 2011 IEEE World Haptics Conference, Istanbul, Turkey, 2011, pp. 323-328

[2] K. Dandekar, B.I. Raju and M.A. Srinivasan: "3-D finite-element models of human and monkey fingertips to investigate the mechanics of tactile sense," Journal of Biomedical Engineering, Vol. 125, No. 5, pp. 682–691, 2003

[3] M. Tada and D.K. Pai," Finger shell: Predicting finger pad deformation under line loading," Proceedings of the Symposium on Haptic Interfaces for Virtual Environment and Teleoperator Systems, pp. 107–112, 2008

[4] A.V. Ho and S. Hirai:" Toward a Platform of Human-Like Fingertip Model in Haptic Environment for Studying Sliding Tactile Mechanism," Proceedings of Robotics: Science and Systems, 2013.

[5] S.A. Mascaro, H.H. Asada:" Measurement of finger posture and threeaxis fingertip touch force using fingernail sensors," IEEE Transactions on Robotics and Automation, vol. 20, no. 1, pp. 26–35, 2004.

[6] A. Ikeda, N. Saito, J. Li, A. Yano and T. Kawazoe, "Wearable finger pad deformation sensor for precise 3D fingertip force estimation," IEEE World Haptics Conference 2019, DM2.07, Tokyo, JAPAN, 9-12 July 2019.

[7] G. Wu et al., "ISB recommendation on definitions of joint coordinate systems … Part II: shoulder, elbow, wrist and hand," J. Biomech., vol. 38, pp. 981-992, 2005.

[8] A. C. Brantley, T. P. Andriacchi, and S. L. Delp, "Prediction of three-directional ground reaction forces during walking using a shoe-sole sensor system and machine learning," IEEE Trans. Neural Syst. Rehabil. Eng., vol. 31, pp. 145-154, 2023.

[9] L. Xiang, M. S. Wong, and J. R. Tenforde, "Integrating personalized shape prediction, biomechanical modeling, and wearables for bone stress prediction in runners," npj Digital Medicine, vol. 5, no. 122, 2022.